Title
Characterization of Dynamic UbR-Proteasome Subcomplexes by In vivo Cross-linking (X) Assisted Bimolecular Tandem Affinity Purification (XBAP) and Label-free Quantitation.

Journal
Molecular & cellular proteomics : MCP, 15(7)

ISSN
1535-9476

Authors
Yu, Clinton
Yang, Yingying
Wang, Xiaorong
et al.

Publication Date
2016-07-01

DOI
10.1074/mcp.m116.058271

Peer reviewed

Characterization of Dynamic UbR-Proteasome Subcomplexes by *In vivo* Cross-linking (X) Assisted Bimolecular Tandem Affinity Purification (XBAP) and Label-free Quantitation*[S]

Clinton Yu‡‡‡, Yingying Yang‡‡‡, Xiaorong Wang‡, Shenheng Guan§, Lei Fang‡, Fen Liu¶, Kylie J. Walters¶, Peter Kaiser‖, and Lan Huang‡**

Proteasomes are protein degradation machines that exist in cells as heterogeneous and dynamic populations. A group of proteins function as ubiquitin receptors (UbRs) that can recognize and deliver ubiquitinated substrates to proteasome complexes for degradation. Defining composition of proteasome complexes engaged with UbRs is critical to understand proteasome function. However, because of the dynamic nature of UbR interactions with the proteasome, it remains technically challenging to capture and isolate UbR-proteasome subcomplexes using conventional purification strategies. As a result, distinguishing the molecular differences among these subcomplexes remains elusive. We have developed a novel affinity purification strategy, *in vivo* cross-linking (*X*) assisted *b*imolecular tandem *a*ffinity *p*urification strategy (XBAP), to effectively isolate dynamic UbR-proteasome subcomplexes and define their subunit compositions using label-free quantitative mass spectrometry. In this work, we have analyzed seven distinctive UbR-proteasome complexes and found that all of them contain the same type of the 26S holocomplex. However, selected UbRs interact with a group of proteasome interacting proteins that may link each UbR to specific cellular pathways. The compositional similarities and differences among the seven UbR-proteasome subcomplexes have provided new insights on functional entities of proteasomal degradation machineries. The strategy described here represents a general and useful proteomic tool for isolating and studying dynamic and heterogeneous protein subcomplexes in cells that have not been fully characterized. ***Molecular & Cellular Proteomics 15: 10.1074/mcp.M116.058271, 2279–2292, 2016.***

Proteasomes are multisubunit protein complexes that are responsible for the degradation of ubiquitinated substrates to maintain cell viability and homeostasis. The 26S proteasome is composed of at least 33 subunits (1–3), which can be divided into two subcomplexes: the 20S catalytic core particle (CP)[1] and the 19S regulatory particle (RP). The 20S CP is responsible for various proteolytic activities, and has a highly conserved "barrel"-like structure consisting of two copies each of 14 nonidentical subunits (α1–7, β1–7), which are arranged into four heptameric rings stacked in the order of $\alpha_7\beta_7\beta_7\alpha_7$ (4, 5). The 19S RP intimately interacts with the 20S CP, regulating its activity. In addition, the 19S RP carries diverse functions including substrate recognition and deubiquitination, protein unfolding, and substrate translocation to the 20S CP for degradation (2, 3, 6–8). In contrast to the highly ordered and stable structure of the 20S CP, the 19S RP appears to be much more flexible and dynamic (3, 9–11). Current structural analyses have revealed that six Rpt subunits of the 19S RP form a hexameric AAA-ATPase ring to associate with the cylinder ends of the 20S CP, and are surrounded by a shell of Rpn subunits (9–11). Apart from the

From the ‡Department of Physiology & Biophysics, University of California, Irvine, California 92697; §Department of Pharmaceutical Chemistry, University of California, San Francisco, California 94143; ¶Protein Processing Section, Structural Biophysics Laboratory, Center for Cancer Research, National Cancer Institute, Frederick, Maryland 21702; ‖Department of Biological Chemistry, University of California, Irvine, California 92697

Received January 12, 2016, and in revised form, April 7, 2016
Published, MCP Papers in Press, April 25, 2016, DOI 10.1074/mcp.M116.058271
Author contributions: L.H. designed research; C.Y., Y.Y., and X.W. performed research; X.W., L.F., F.L., K.J.W., and P.K. contributed new reagents or analytic tools; C.Y., Y.Y., S.G., and L.H. analyzed data; C.Y. and L.H. wrote the paper.

[1] The abbreviations used are: CP, 20S catalytic core particle; UbR, ubiquitin receptor; XBAP, *In vivo* Cross-linking (*X*) Assisted *B*imolecular Tandem *A*ffinity *P*urification; RP, 19S regulatory particle; UPS, ubiquitin proteasome system; UBL, ubiquitin-like domain; UBA, ubiquitin associated domain; AP-MS, affinity purification mass spectrometry; PIP, proteasome interacting proteins; HB, histidine and biotin tag; QTAX, *q*uantitative analysis of *t*andem *a*ffinity purified in vivo cross-linked (x) proteasome complexes; HF, histidine and FLAG tag; LC MS/MS, liquid chromatography tandem mass spectrometry; TB, TEV cleavage sequence-Biotin tag; Co-IP, co-immunoprecipitation; LFQ, label free quantitation.

19S RP, the 20S proteasome can be activated by three other known regulatory protein complexes, *i.e.* PA28α/β (also known as REG and the 11S regulator), PA28γ/REGγ, and PA200/Blm10, to form distinct functional subspecies of proteasomes (1, 2). In contrast to the 19S RP, these proteasome activator complexes do not have ATPase activity and can only assist in ubiquitin-independent protein degradation with varied proteolytic cleavage specificities.

Delivery of ubiquitinated substrates to the 26S proteasome is an important regulatory step in the ubiquitin proteasome system (UPS) (2, 3). It is generally believed that the initial recognition of substrates by the proteasome is mediated by the substrate-attached polyubiquitin chain (1–3). Ubiquitin receptors (UbRs) are a group of proteins that can recognize and bind polyubiquitin chains (2, 3, 12). Five types of UbRs have been well recognized to be associated with proteasomal degradation, including the two proteasome subunits Rpn10 (13) and Rpn13/ADRM1 (14), and three "shuttling factors," Rad23, Dsk2, and Ddi1 (2, 3) (Table I). In humans, the non-proteasome receptor families *RAD23* and *DDI1* are each comprised of two distinct isoforms, *i.e.* hHR23A, hHR23B, Ddi1 and Ddi2. Five genes have been identified for the *DSK2* family in humans encoding ubiquilin proteins, *i.e. UBQLN1 (a.k.a PLIC-1), UBQLN2 (a.k.a. PLIC-2), UBQLN3, UBQLN4 (a.k.a. A1Up, UBIN, CIP75*), and *UBQLNL* (15). Each of the UbR isoforms has been suggested to carry different specificities and functions (2, 15–17). Interestingly, human UbRs have been implicated in various human diseases. For example, the human Rpn13/ADRM1 gene is overexpressed in lung, ovarian, colon, liver, kidney, bladder, and stomach cancers (18), and ADRM1 amplification in ovarian cancers correlates significantly with shorter time to recurrence and death (19). The Rpn13/ADRM1 inhibitor RA190 inhibits proteasome functions, triggers apoptosis, and restricts cancer growth in mice xenografts (20), and similar effects were observed with an Rpn13/ADRM1-targeting peptoid inhibitor (21). hHR23B has been identified as a candidate cancer biomarker that governs the response and sensitivity of tumor cells to HDAC inhibitors (22, 23). Mutations in *UBQLN1* and *UBQLN2* have been linked to multiple neurodegenerative disorders including Alzheimer's and amyotrophic lateral sclerosis (ALS) (15). Given their importance in the UPS and human pathologies, deeper understanding of the mechanisms underlying proteasomal degradation through UbR pathways would provide a molecular basis for better therapeutics with higher selectivity/specificity by targeting subpopulations of proteasome substrates.

In comparison to non-proteasome UbRs, Rpn10 and Rpn13/ADRM1 possess unique interaction domains for binding to ubiquitin. Although Rpn10 recognizes ubiquitin chains via its helical ubiquitin-interacting motif (UIM) (24), Rpn13/ADRM1 uses a globular Pleckstrin-like receptor for ubiquitin (Pru) domain (14, 25). During proteasome assembly, Rpn10 attaches primarily to the lid and stabilizes the lid-base interaction (26), whereas Rpn13 appears to assemble into the proteasome exclusively through Rpn2 (25, 27, 28). The non-proteasome UbRs are referred to collectively as the UBL (ubiquitin-like)/UBA(ubiquitin associating) receptors and are not integral proteasome subunits, but substoichiometric components of purified proteasomes. Each UBL/UBA receptor contacts the proteasome through its UBL domain, whereas the ubiquitin chain is bound through one or more UBA domains. UBA/UBL receptors bind to proteasomes by interacting with Rpn1 (29), Rpn10 and Rpn13 (14, 30). In mammalian cells, the UBA/UBL receptors have also been shown to interact with proteasomes via Rpn10 (31, 32) and other components of the 19S complex (33). Although the known UbRs functionally overlap substantially, at least in part, and cooperate in mediating proteasomal degradation (14, 34, 35), it is clear that they exert distinct effects on substrate stability *in vivo* (2, 3, 16, 35). Although it is clear that proteasomes exist as heterogeneous populations in cells (1, 36–38), it is uncertain why so many ubiquitin receptors exist, whether each UbR binds to a unique subpopulation of proteasome complexes, and whether this complexity translates into differential substrate stability and receptor specificity. In order to understand how the proteasome selects different types of target proteins and how UbR substrate specificity is controlled *in vivo*, it is necessary to characterize UbR-proteasome subcomplexes and determine their quantitative differences in subunit composition.

Affinity purification coupled with mass spectrometry (AP-MS) has demonstrated its effectiveness in isolating native complexes under various physiological conditions for determining their subunit composition, posttranslational modifications, interaction networks and structures (39–42). Current AP-MS strategies typically rely on affinity purification with a specific bait through one-step or two-step purification processes. Although tandem affinity purification allows the purification of protein complexes with higher specificity and lower background, weak interactions are often lost because of extended procedures. In comparison, single-step AP-MS strategies are more advantageous in preserving protein interactions of protein complexes, especially weak ones, because of fewer washing steps. Regardless of differences in purification specificity, both strategies often lead to co-purification of heterogeneous protein complexes owing to direct or indirect protein association under AP-MS experimental conditions. In order to improve homogeneity of purified protein complexes, it has been suggested to tag two distinct subunits for sequential isolation of protein complexes containing the two desired components (43). However, the application of this approach in analyzing protein subcomplexes, particularly dynamic ones, needs to be demonstrated.

To effectively isolate proteasome complexes from mammalian cells, we previously developed a new purification strategy based on a derivative of the His-Bio (HB) tag which was fused to a proteasome subunit (44, 45). This method allowed facile purification of functional human proteasome complexes un-

der native conditions in a single-step (45, 46), in which proteasome subunits and proteasome interacting proteins (PIPs) were captured and analyzed. During these analyses, we have determined that three UbR proteins, *i.e.* Rpn13/ADRM1, hHR23B, and Ubqln1, bind to proteasomes dynamically with fast on/off rates (46). Therefore, their co-purification with proteasomes is highly dependent on experimental conditions and furthermore, the interactions of hHR23B and Ubqln1 with proteasomes have not been consistently detected when conventional AP-MS strategies were applied. To capture protein-protein interactions of all natures in a single analysis, we have developed a QTAX (*Q*uantitative analysis of *t*andem affinity purified *in vivo* c*x*oss-linked (*x*) protein complexes) strategy by integrating *in vivo* chemical cross-linking, HB-based tandem affinity purification of protein complexes under fully denaturing conditions and quantitative mass spectrometry (47, 48). Our results have demonstrated that *in vivo* cross-linking can extend the identification of interacting proteins by capturing weak or transient interactors in addition to stable ones, thus allowing effective co-purification of the known UbRs with yeast proteasomes (48). The recent development of the newly developed membrane-permeable, MS-cleavable and enrichable cross-linker Azide-A-DSBSO enables the determination of subunit-subunit interaction contacts of *in vivo* cross-linked HB-tagged proteasome complexes by multistage tandem mass spectrometry (49). Clearly, it is advantageous to couple HB-tag based tandem affinity purification with cross-linking mass spectrometry to provide the unique capability of tandem affinity purification of proteins under fully denaturing conditions (44, 47). This enables the elimination of nonspecific background to enhance the detection of cross-linked products associated with the bait (44, 47, 48, 50, 51). Although the composition of protein complexes resulting from denaturing purification can be readily determined, subunit stoichiometry can be misrepresented because of variance in protein cross-linking efficiency, leading to varying protein absolute abundances. Previously, it has been shown that mild cross-linking can be coupled with native purification to preserve protein interactions (52–54). In order to isolate UbR-proteasome subcomplexes and determine their quantitative differences in proteasome subunit composition, we have developed a novel affinity purification strategy XBAP, *i.e. in vivo* cross-linking (*X*) assisted *b*imolecular tandem *a*ffinity *p*urification. With XBAP, we were able to analyze the proteasomes present in the seven selected UbR-proteasome complexes, and thus understand the proteasomal populations actively engaged in proteolysis of ubiquitinated proteins. Importantly, the novel integrated strategy developed here embodies a valuable tool to better characterize protein subcomplexes, stable or dynamic, yielding biologically relevant information that cannot be easily obtained using existing approaches.

EXPERIMENTAL PROCEDURES

Chemicals and Reagents—General chemicals for buffers and cell culture media were purchased from Fisher (Waltham, MA) or VWR (Radnor, PA). ImmunoPure streptavidin, HRP-conjugated antibody and Super Signal West Pico chemiluminescent substrate were from Pierce Biotechnology (Rockford, IL). Sequencing grade trypsin was purchased from Promega Corp. (Madison, WI), and anti-FLAG was from Sigma-Aldrich (St. Louis, MO).

Plasmid and Cloning—Construction of HisFLAG-UbR-pQCXIP plasmid: for HisFLAG-UbR-pQCXIP, HisFLAG fragment was obtained by annealing using these two primers: forward 5′-GGCCGCATGAGGGGTTCACATCATCACCACCATCATGACTACAAAGACGATGACGACAAGTTAAT-3′; reverse 5′-TAACTTGTCGTCATCGTCTTTGTAGTCATGA TGGTGGTGATGATGTGAACCCCTCATGC-3′. The annealing product was directly inserted into NotI and PacI digested pQCXIP to get pQCXIP-HisFlag. Rpn13/ADRM1 fragment was PCR amplified from ADRM1 containing plasmid from KJW using the following primers: forward, 5′-TTAATTAACACGACCTCAGGCGCGCTCTTTCCAAG-3′; reverse, 5′-GAATTCTCAGTCCAGGCTCATGTCCTCCTCTTC-3′. The obtained PCR fragment was confirmed by DNA sequencing, digested by PacI and EcoR I and inserted into the same treated pQCXIP-HisFlag to get pQCXIP-HisFlag-ADRM1. For the rest of pQCXIP-HisFlag-UbR, UbR fragments were PCR amplified from corresponding UbR containing plasmids from KJW using the following forward and reverse primers: Rpn10: forward, 5′-TTAATTAACGTGTTGGAAAGCACTATGGTGTGTGTG-3′; reverse, 5′-GAATTCTCACTTCTTG TCTTCCTCCTTCTTGTCC-3′. hHR23b: forward, 5′-TTAATTAAC CAGGTCACCCTGAAGACCCTCCAGC-3′; reverse, 5′-GAATTCTCAATCTTCA TCAAAGTTCTGCTGTAGAAG-3′. Ddi1: forward, 5′-TTAATTAACATGCTGATCA CCGTGTACTG CGTGC-3′; reverse, 5′-GAATTCTTAATGTTCTTTTCGTCCTG AATCCATG-3′. Ddi2: forward, 5′- TTAATTAACATGCTGCTCACCGTGTACTGTGTG-3′; reverse, 5′-GAATTCTCATGGCTTCTGACGCTCTGCATC-3′. Ubqln1: forward, 5′-TTA ATTAACGCCGAGAGTGGTGAAAGCGGCGGTC-3′; reverse, 5′-GGATCCCTA TGATGG CTGGGAGCCCAGTAACC-3′. Ubqln2: forward, 5′-TTAATTAACGCTGAGA ATGGCGAGAGCAGCGGCC-3′; reverse, 5′-GAATTCTTACGATGGCTGGGAGCCCA GCAGCC-3′. The obtained UbR PCR fragments were confirmed by DNA sequencing, digested by PacI and EcoR I (BamH1 for Ubqln1) and inserted into the same treated pQCXIP-HisFlag-Rpn13/ADRM1 to get pQCXIP-HisFlag-UbR.

For construction of Rpn11-TB-pQCXIH, Rpn11 was digested from Rpn11-HTBH-pQCXIP by NotI and PacI and inserted into pQCXIH vector to obtain Rpn11-pQCXIH. Then TB fragment was PCR amplified from HTBH-pQCXIP using the following primers: forward, 5′-TTAATTAAC GACTACGATATACCCACAACCGC-3′; reverse, 5′-GAATTCCTA AACGCCGATCTTGATTAGACCTTG-3′. The obtained fragment was confirmed by DNA sequencing, digested by PacI and EcoR I and inserted into the same treated Rpn11-pQCXIH to get Rpn11-TB-pQCXIH. These constructs contain CMV promoters.

Generation of 293$^{HF\text{-}UbR/Rpn11\text{-}TB}$ Stable Cell Lines—The procedure for making the retrovirus was similar to that reported previously (45). Because we are using retroviral vectors from Clontech, the details on retroviral gene transfer can be found at (http://www.com/US/Products/Viral_Transduction/Retroviral_Vector_Systems/ibcGetAttachment.jsp?cItemId=17555&fileId=6684076&sitex=10020:22372:US). Briefly, a 293 GP2 cell line was co-transfected with pQCXIP-Rpn11-TB and pQCXIH-HF-UbR. Retrovirus was produced and released to the medium between 36 h to 96 h after transfection. Retrovirus containing medium was used to transduce 293 cells, which were subsequently selected with puromycin and hygromycin to establish the stable cell lines co-expressing Rpn11-TB and HF-UbR, *i.e.* 293$^{HF\text{-}UbR/Rpn11\text{-}TB}$. In total, seven dual-bait stable cell lines were generated in this work.

Experimental Design and Statistical Rationale—To isolate UbR-proteasome subomplexes for XBAP experiments, $293^{HF\text{-}UbR/Rpn11\text{-}TB}$ cells were grown to confluence in DMEM medium containing 10% FBS and 1% Pen/strep, then trypsinized and washed 3 times with PBS buffer. The cell pellets were collected and lysed in buffer A (100 mM sodium chloride, 50 mM sodium phosphate, 10% glycerol, 5 mM ATP, 1 mM DTT, 5 mM $MgCl_2$, 1X protease inhibiter (Roche), 1X phosphatase inhibitor, 0.1% Nonidet P-40, pH 7.5). *In vivo* formaldehyde cross-linking of intact cells was carried out in PBS buffer at room temperature for 10 min and quenched with a final concentration of 0.125 M glycine. The cross-linked cells were pelleted and washed with PBS, then lysed in native lysis buffer (50 mM Tris, 100 mM NaCl, 1X protease inhibitor, 10% Glycerol, 1 mM DTT, 5 mM ATP, 5 mM $MgCl_2$). The lysates were centrifuged at 13,000 rpm for 15 min to remove cell debris and the supernatant was incubated with anti-FLAG M2 affinity gel for 3 h at 4 °C based on the manufacturer's protocol. The FLAG beads were then washed with 30 bed volumes of the lysis buffer, followed by a final wash with 15 bed volumes of TBS buffer (50 mM Tris-HCl, 100 mM NaCl, 5 mM ATP, 10% glycerol, pH7.4). The bound proteins were eluted using 150 μg/ml of 3X FLAG peptide in TBS buffer. The resulting eluent was subsequently bound with streptavidin beads for 2 h at 4 °C, which was then washed with 50 bed volumes of TBS buffer and 10 bed volumes of 25 mM NH_4HCO_3 (45). To minimize sample loss, bound protein samples were directly subjected to subsequent trypsin digestion and mass spectrometric analysis. Each purification experiment was repeated once to obtain two biological replicates to assess reproducibility.

The isolated UbR-proteasome complexes bound on streptavidin beads were digested with trypsin as described (50). Liquid chromatography and tandem mass spectrometry (LC MS/MS) was carried out using an LTQ-Orbitrap XL MS (ThermoFisher Scientific) coupled on-line with an EASY NanoLC 1000 system (ThermoFisher Scientific) as previously described (51). Each cycle of an MS/MS experiment includes one MS scan in FT mode (350–1400 *m/z*, resolution of 60,000 at *m/z* 400) followed by data-dependent MS2 scans in the LTQ with normalized collision energy at 35% on the top ten peaks.

To identify proteins through database searching, monoisotopic masses of parent ions and corresponding fragment ions, parent ion charge states, and ion intensities from LC MS/MS spectra were first extracted based on the Raw_Extract script from Xcalibur v2.4 as described (51). The data were searched using the Batch-Tag within the developmental version (v 5.10.0) of Protein Prospector against a decoy database consisting of a normal Swissprot database concatenated with its randomized version (SwissProt.2014.12.4.random.concat with total 20,196 protein entries searched). Homo Sapiens was selected as the species. The mass accuracy for parent ions and fragment ions were set at $\pm$ 20 ppm and 0.6 Da, respectively. Trypsin was set as the enzyme and a maximum of two missed cleavages were allowed. Protein N-terminal acetylation, methionine oxidation, and N-terminal conversion of glutamine to pyroglutamic acid were selected as variable modifications. The proteins were identified by at least two peptides with a false-positive rate $\leq$ 0.5%. Each purification was analyzed by MS in duplicate (*i.e.* two technical replicates), totaling 28 LC MS/MS runs. Commonly known purification background, such as ribosomal proteins, actins, spectrin and tubulin, was excluded from the final list (45, 46). All the raw data have been deposited at http://massive.ucsd.edu/ProteoSAFe/status.jsp?task=d0d521386f854c52810f2cefca16ef92 (password: UbR040716).

Label-free Based Quantitative Comparison of UbR-proteasome Subcomplexes—Label-free quantitation was carried out using MaxQuant as described (55, 56). Briefly, the Raw files were searched using MaxQuant (v. 1.5.0.0) against human complete proteome sequences obtained from UniProt (version from November 2012). The first search peptide tolerance was set to 20 ppm, with main search peptide tolerance set to 4.5 ppm. For quantitation, intensities were determined as the full peak volume over the retention time profile. Intensities of different isotopic peaks in an isotope pattern were always summed up for further analysis. "Unique plus razor peptides" was selected as the degree of uniqueness required for peptides to be included in quantification. The resulting LFQ values for each identified protein by MaxQuant were used for comparing protein relative abundance among different samples.

Proteasome Proteolytic Activity Assay—In-solution proteolytic activity assays for human proteasomes were performed with the fluorogenic peptide substrates SUC-LLVY-AMC, SUC-LLE-AMC, and SUC-ARR-AMC, as described previously (45). Briefly, 10 μl of each samples were incubated with 100 μM of substrate for 30 min at 37 °C, then the reaction was quenched by 1% SDS, the fluorescence were measured at an excitation of 380 nm and emission of 460 nm. The concentration of the total protein was determined by Nano1000. The proteasome activities were normalized to the total protein. Three biological replicates were performed, and each of them was analyzed with three technical replicates.

RESULTS

Developing a New Dual-bait Strategy for Effective Isolation of UbR-proteasome Complexes—In order to determine interactions of specific UbRs with proteasome complexes, we have developed a new bimolecular affinity purification strategy enabling robust isolation of distinct UbR-proteasome complexes. One of the key elements in this strategy is the construction of two affinity tags that can be fused to two selected baits for sequential purification of protein subcomplexes containing the two desired baits, *i.e.* a UbR protein and a proteasome subunit. In order to permit affinity purification under both native and denaturing conditions, we decided to split the HB tag into a HF (His_6-FLAG) and a TB (TEV-biotin) tag for respective tagging of a UbR and of a proteasome subunit (Fig. 1A). The addition of the FLAG tag to the hexahistidine tag is to improve affinity purification under native conditions. Because of its specificity, a histidine tag is better suited for denaturing than native purifications. The TB tag consists of a TEV cleavage site and a signaling peptide for *in vivo* biotinylation, the same as that found in the HTBH tag (44, 45). This dual-tagging strategy is versatile and advantageous as the combination of the HF and TB tags permits effective protein purification under both native and denaturing conditions. In this work, we attempted to target the five well-known types of human UbRs for our studies (Table I). Among the five ubiquilin proteins, Ubqln1, Ubqln2 and Ubqln4 have been found in all tissues, whereas Ubqln3 and Ubqlnl appear to be enriched in testis (http://www.proteinatlas.org/). In comparison, Ubqln1 and Ubqln2 have the highest levels of expression among all ubiquilin genes in most mouse and human tissues (15), and have been implicated in several neurodegenerative disorders (15, 57, 58). Therefore, we have selected these two ubiquilins for this work. In order to generate a full picture of UbR-proteasome interactions, a total of eight human UbR proteins (*i.e.* Rpn10, Rpn13/ADRM1, hHR23A, hHR23B, Ddi1, Ddi2, Ubqln1, and Ubqln2) were selected for tagging. As a result, we were successful in creating seven HF-UbR con-

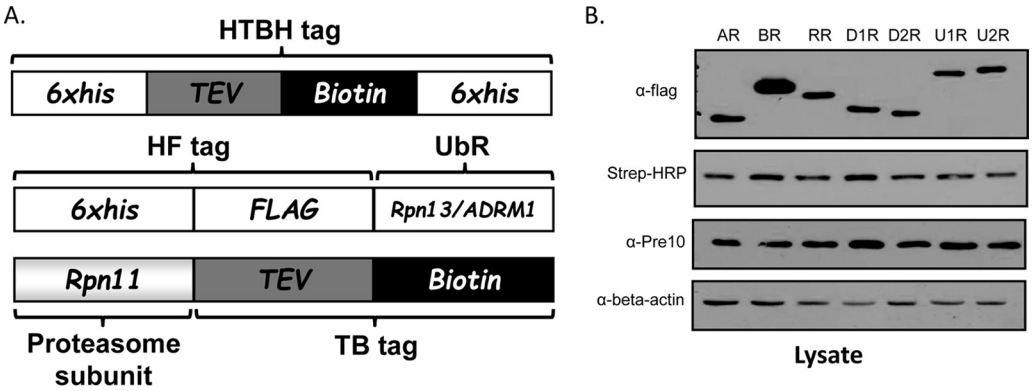

FIG. 1. **The Split-tag strategy for the isolation of UbR-porteasome complexes.** *A*, Constructs of HTBH tag, HF-Rpn13/ADRM1; and Rpn11-TB; *B*, Protein levels of seven HF-tagged UbRs in their corresponding stable 293 cells in which a HF-UbR and Rpn11-TB were co-expressed. The seven cells are termed as AR ($293^{\text{HF-Rpn13/ADRM1\_Rpn11-TB}}$), RR ($293^{\text{HF-Rpn10\_Rpn11-TB}}$), BR (($293^{\text{HF-hHR23B\_Rpn11-TB}}$), D1R($293^{\text{HF-Ddi1\_Rpn11-TB}}$), D2R($293^{\text{HF-Ddi2\_Rpn11-TB}}$), U1R($293^{\text{HF-Ubqln1\_Rpn11-TB}}$), U2R($293^{\text{HF-Ubqln2\_Rpn11-TB}}$). UbRs were detected by antibody α-FLAG, and Rpn11 was probed by strep-HRP. A 20S subunit (Pre10/α7) was also probed. Beta actin served as a loading control.

TABLE I
The five selected UbR families

UbR Family	Yeast Protein	Human Protein	Selected for XBAP experiments
Rpn10	Rpn10	Rpn10/S5a	√
Rpn13	Rpn13	Rpn13/ADRM1	√
Rad23	Rad23	hHR23A	√[a]
		hHR23B	√
Dsk2	Dsk2	Ubqln1	√
		Ubqln2	√
		Ubqln3	-
		Ubqln4	-
		Ubqlnl	-
Ddi1	Ddi1	Ddi1	√
		Ddi2	√

[a] Gene expression was not successful.

structs, all except hHR23A. Rpn11, one of the essential 19S proteasome subunits, was selected for co-expression with the UbRs, because of its critical importance in proteasomal degradation and its extensive use as a bait for isolating proteasomes both in human and yeast (45, 47, 59, 60). To isolate UbR-Rpn11 complexes, seven 293 cell lines (*i.e.* $293^{\text{HF-UbR\_Rpn11-TB}}$) stably co-expressing Rpn11-TB and a HF-UbR were generated by retrovirus infection and antibiotic selection in the same way as described (45): $293^{\text{HF-Rpn13/ADRM1\_Rpn11-TB}}$, $293^{\text{HF-Rpn10\_Rpn11-TB}}$, $293^{\text{HF-hHR23B\_Rpn11-TB}}$, $293^{\text{HF-Ddi1\_Rpn11-TB}}$, $293^{\text{HF-Ddi2\_Rpn11-TB}}$, $293^{\text{HF-Ubqln1\_Rpn11-TB}}$, and $293^{\text{HF-Ubqln2\_Rpn11-TB}}$. For simplicity, we have termed these cells in short as AR, RR, BR, D1R, D2R, U1R, and U2R accordingly. Expression levels of HF-UbR and Rpn11-TB from seven cell lines were examined using immunoblotting (Fig. 1*B*). As shown, HF-tagged UbR proteins displayed similar expression levels, and their expression did not change Rpn11-TB abundance level in dual-bait cells.

Purification and Characterization of UbR-proteasome Complexes—Given the dynamic nature of UbR interactions with proteasomes, it is technically challenging to preserve UbR-proteasome complexes using conventional affinity purification strategies under native conditions, even with one-step purification approaches (45, 46). Indeed, our initial analysis revealed that it was difficult to consistently obtain UbR-proteasome subcomplexes with bimolecular tandem affinity purification by isolating HF-tagged UbR first and then TB-tagged Rpn11 subsequently under native conditions. In order to maintain the integrity of UbR-proteasome subcomplexes, we have developed a novel integrated strategy, XBAP, *i.e. in vivo* Cross-linking (*X*) assisted *B*imolecular tandem *A*ffinity *P*urification (Fig. 2). This method incorporates *in vivo* formaldehyde (FA) cross-linking with sequential affinity purification using two differentially tagged baits. The key facet is to introduce a very mild cross-linking condition that is sufficient enough to ensure the stabilization of dynamic interactors but not to compromise the intactness of proteasome complexes for purification under native conditions and subsequent MS analysis. To test the effect of low formaldehyde cross-linking on proteasome integrity, we have measured proteasome activities in cell lysates using fluorogenic peptide substrates (Fig. 3). As shown, the three selected proteolytic activities were at their highest when cells were treated with 0.05% formaldehyde prior to cell lysis. These results further confirm that proteasomes are highly dynamic entities in cells and suggest that low level cross-linking can be beneficial for stabilizing proteasome structure and function during cell lysis prior to affinity purification, in good agreement with a previous report (54). To further evaluate the effect of mild cross-linking on subsequent purification and MS analysis, we purified proteasomes using HF-Rpn13/ADRM1 as the bait from $293^{\text{HF-Rpn13/ADRM1\_Rpn11-TB}}$ cells. The abundance of proteasome subunits was not significantly affected by mild formaldehyde *in vivo* cross-linking (supplemental Fig. S1*A*). However, *in vivo* cross-linking helped the capture of weakly bound known PIPs, which were then identified with increased abundance (supplemental Fig. S1*B*). Therefore, *in vivo* cross-linking with 0.05% formaldehyde has been incorporated in all of

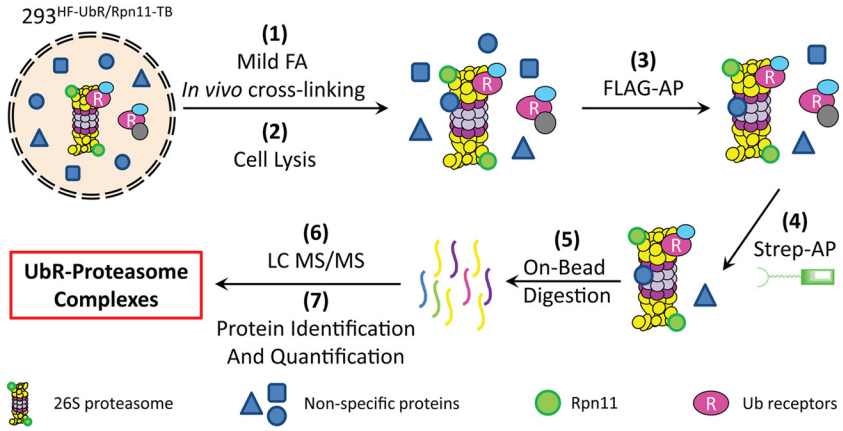

FIG. 2. **The general XBAP-MS strategy for analyzing UbR-proteasome complexes from stable 293 cells expressing a HF-tagged UbR and a TB tagged proteasome subunit (*i. e.* Rpn11-TB) by label-free based MS quantitative analysis.** Note: FLAG-AP: FLAG based affinity purification; Strep-AP: affinity purification of biotin-tagged proteins by binding to streptavidin beads.

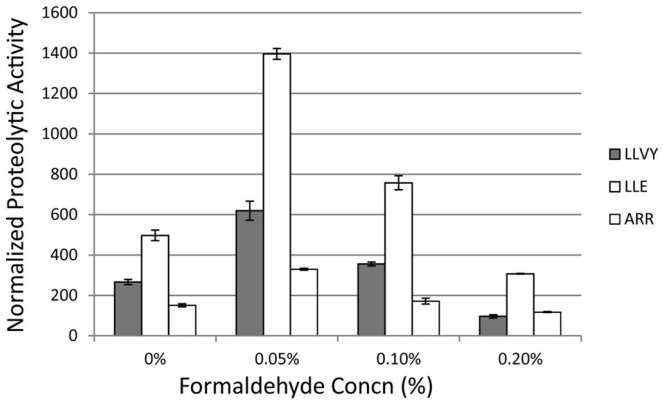

FIG. 3. **The effects of *in vivo* formaldehyde treatment on three proteolytic activities of the human 26S proteasome using an in-solution assay with flurogenic peptide substrates.** Chymotryptic activity-LLVY; Caspase-like activity-LLE; Tryptic activity-ARR. Three biological replicates were performed, each yielding nearly identical results. For simplicity, the technical replicates for a single biological replicate are shown. Error bars represent the standard deviation between three technical repeats.

our XBAP experiments described below (Fig. 2). To better assess subunit composition and abundance, it is noted that UbR-proteasome complexes are purified under native conditions to better preserve the integrity of protein complexes. This is especially important when two different baits are used sequentially and a label-free quantitative method is employed. The two-step affinity purification is accomplished by FLAG-tag based affinity purification followed by binding to streptavidin beads. The purification process was evaluated by immunoblotting as shown in supplemental Fig. S2. As illustrated, low formaldehyde cross-linking did not interfere with native affinity purification as tagged proteins were efficiently bound to corresponding resins for all cells tested. Although the TEV cleavage step is effective and can be performed at the last purification step, we decided to directly digest the complexes bound on streptavidin beads to eliminate sample loss and minimize experimental variance. The resulting digests were subjected to LC MS/MS analysis. In this study, we have repeated the purification of UbR-proteasome subcomplexes and each sample was run twice by LC MS/MS, thus yielding two biological replicates with two technical replicates respectively for each UbR sample. In total, 28 LC MS/MS runs were analyzed in parallel for database searching and results comparison. In this work, we only considered proteins that were identified with a minimum of two unique peptides and reproducibly identified in both biological replicates. The detailed results on protein identification are summarized in supplemental Table S1. In all experiments, 32 core proteasome subunits were co-purified in UbR-proteasome complexes, including eighteen 19S RP subunits (*i.e.* Rpt1–6, Rpn1–3, and Rpn5–13) and fourteen 20S CP subunits (*i.e.* α1-α7 and β1-β7). Because ubiquitin receptors deliver substrates to the proteasome, they specifically associate with the subpopulation of proteasomes that is important for degradation of ubiquitinated proteins. Our results imply that UbR-bound proteasomes have the same subunit composition, suggesting that the core functional entity remains intact regardless of how substrates are transported to proteasomes for degradation.

Quantitative Comparison of UbR-proteasome Complexes—In order to further assess UbR-proteasome complexes, we have carried out label-free quantitative analysis using MaxQuant (55, 56). To compare components of the seven selected UbR-proteasome complexes, LFQ values for each identified protein in each sample were obtained (supplemental Table S2*A*) and normalized to their respective baits (supplemental Table S2*B*), allowing comparison of relative protein abundances among different samples. Although core subunit composition is the same for UbR-proteasome complexes, the amount of proteasomes associated with each UbR appears to be different. Fig. 4 displays the abundance heatmap of 32 core proteasome subunits present in the seven UbR-proteasome complexes. Given the same amount of baits, it seems that Rpn13/ADRM1 binds to the highest amount of the 26S pro-

Name	AR_FSIP	RR_FSIP	BR_FSIP	D1R_FSIP	D2R_FSIP	U1R_FSIP	U2R_FSIP
Rpt1	6.4	3.4	3.2	1.5	0.5	1.8	1.4
Rpt2	4.9	2.5	2.3	0.8	0.4	1.5	0.9
Rpt3	7.0	4.1	3.0	1.3	0.5	2.0	1.2
Rpt4	4.4	2.3	1.9	0.8	0.3	1.1	0.8
Rpt5	4.1	2.4	1.7	0.8	0.3	1.2	0.9
Rpt6	5.8	3.2	2.5	1.2	0.5	1.8	1.1
Rpn1	9.6	5.3	4.9	1.8	0.8	2.9	1.7
Rpn2	7.1	3.8	3.3	1.4	0.6	2.1	1.4
Rpn3	8.2	4.1	4.2	1.6	0.7	2.2	1.6
Rpn5	4.1	2.3	1.9	0.9	0.4	1.5	0.8
Rpn6	5.7	2.8	2.8	1.0	0.5	1.6	1.1
Rpn7	5.3	2.7	2.2	1.2	0.4	1.2	1.0
Rpn8	3.1	1.5	1.3	0.5	0.2	0.7	0.5
Rpn9	4.5	2.4	1.8	0.9	0.4	1.1	0.8
Rpn10	1.9	1.0	1.1	0.2	0.2	0.4	0.2
Rpn11	1.6	0.8	0.9	0.3	0.2	0.6	0.3
Rpn12	1.5	0.8	0.8	0.3	0.1	0.5	0.3
Rpn13	1.0	0.5	0.5	0.4	0.1	0.3	0.1
alpha1	2.3	1.1	1.1	0.4	0.2	0.7	0.4
alpha2	1.8	1.0	0.8	0.2	0.2	0.6	0.3
alpha3	1.8	0.9	0.9	0.3	0.1	0.6	0.4
alpha4	3.5	1.8	1.6	0.8	0.2	0.9	0.9
alpha5	2.6	1.3	1.1	0.4	0.2	0.7	0.5
alpha6	4.2	2.2	1.9	1.0	0.3	1.2	1.0
alpha7	2.8	1.3	1.2	0.6	0.2	0.8	0.5
beta1	1.7	0.9	0.9	0.6	0.1	0.5	0.5
beta2	2.1	1.2	1.0	0.5	0.2	0.7	0.5
beta3	0.8	0.4	0.4	0.1	0.1	0.3	0.1
beta4	1.1	0.5	0.5	0.2	0.1	0.3	0.2
beta5	4.2	1.8	1.9	1.0	0.3	1.1	0.8
beta6	2.2	1.0	1.0	0.4	0.2	0.6	0.4
beta7	1.7	0.9	0.7	0.2	0.1	0.6	0.2

FIG. 4. **Heatmap of proteasome subunit abundance in the seven UbR-proteasome complexes based on average normalized LFQ values obtained from MaxQuant.**

teasome holocomplex, whereas Ddi2 associates with the least amount of the 26S. This finding indicates that UbRs are present in proteasome complexes with different stoichiometries. Although Rpn13/ADRM1 and Rpn10 are inherent core proteasome subunits, the amount of proteasomes co-purified with Rpn13/ADRM1 is about twice that of Rpn10-associated proteasomes, implying that stoichiometry of Rpn13/ADRM1 is different from that of Rpn10 in the 26S holocomplex. This is in good agreement with recent reports suggesting that Rpn13/ADRM1 only exists as one copy in the 26S holocomplex, whereas other subunits including Rpn10 are present as two copies in the complex (61). Collectively, these results further suggest compositional and functional asymmetry of the 26S proteasome in processing ubiquitinated substrates, as Rpn13/ADRM1 is only present in one of two 19S RPs comprising the 26S holocomplex.

Among the five selected non-proteasome UbRs, hHR23B appears to bind to the highest amount of proteasome, at a level similar to Rpn10, suggesting that hHR23B may be the major shuttling factor for ubiquitinated substrates. In comparison to hHR23B, Ddi1, Ubqln1, and Ubqln2 copurified about 50% less proteasome. Surprisingly, Ddi2 captured the least amount of proteasomes based on bait-normalized LFQ values (supplemental Table S2*B*), implying that more proteasome-free Ddi2 may be present in cells. Together, our results suggest that UbRs more likely interact with proteasomes differently because of their specific roles in the recognition and delivery of protein substrates.

To determine whether the core proteasome subunits have similar stoichiometry among the seven UbR-proteasome complexes, we evaluated their relative abundances based on average bait-normalized LFQs. In total, six pair-wise correlation plots were generated using both proteasome subunits and their associated proteins identified in compared samples (supplemental Table S1), in which the AR sample (*i.e.* Rpn13/ADRM1-Rpn11 complex) served as the reference for each comparison. As shown in Fig. 5, a linear relationship was found in all pair-wise comparisons with a great correlation coefficient ($R^2 > 0.95$). These results indicate that proteasome subunits have similar stoichiometry in all UbR-proteasome complexes, further confirming the conserved integrity of the 26S holocomplex in its heterogeneous subpopulations.

Comparison of UPS Components in UbR-proteasome Complexes—Apart from core proteasome subunits, proteasome interacting proteins (PIPs) were identified in UbR-proteasome complexes. A total of 39 PIPs were identified from all experiments, which are distributed as follows: 18 (AR), 18 (RR), 10 (BR), 1 (D1R), 30 (D2R), 1 (U1R) and 1 (U2R). Their

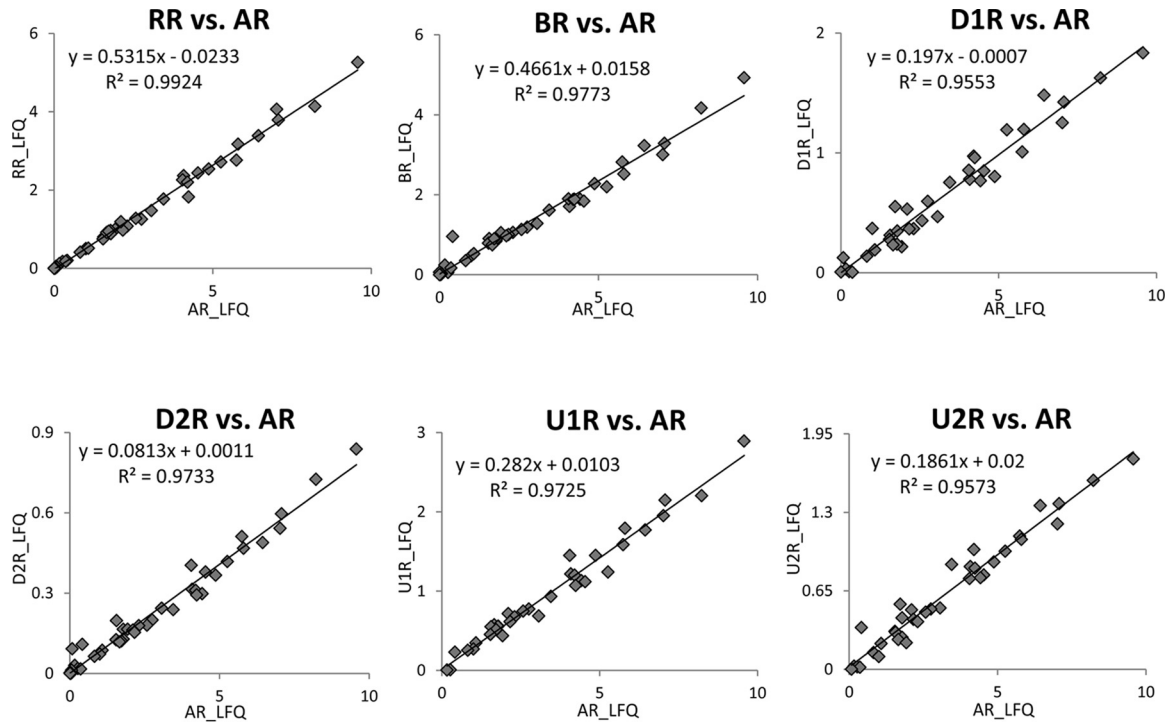

FIG. 5. **Pair-wise correlation plots of LFQ values of proteasomal components in the seven UbR-proteasome complexes, in which RR, BR, D1R, D2R, U1R, U2R were compared with AR sample respectively.**

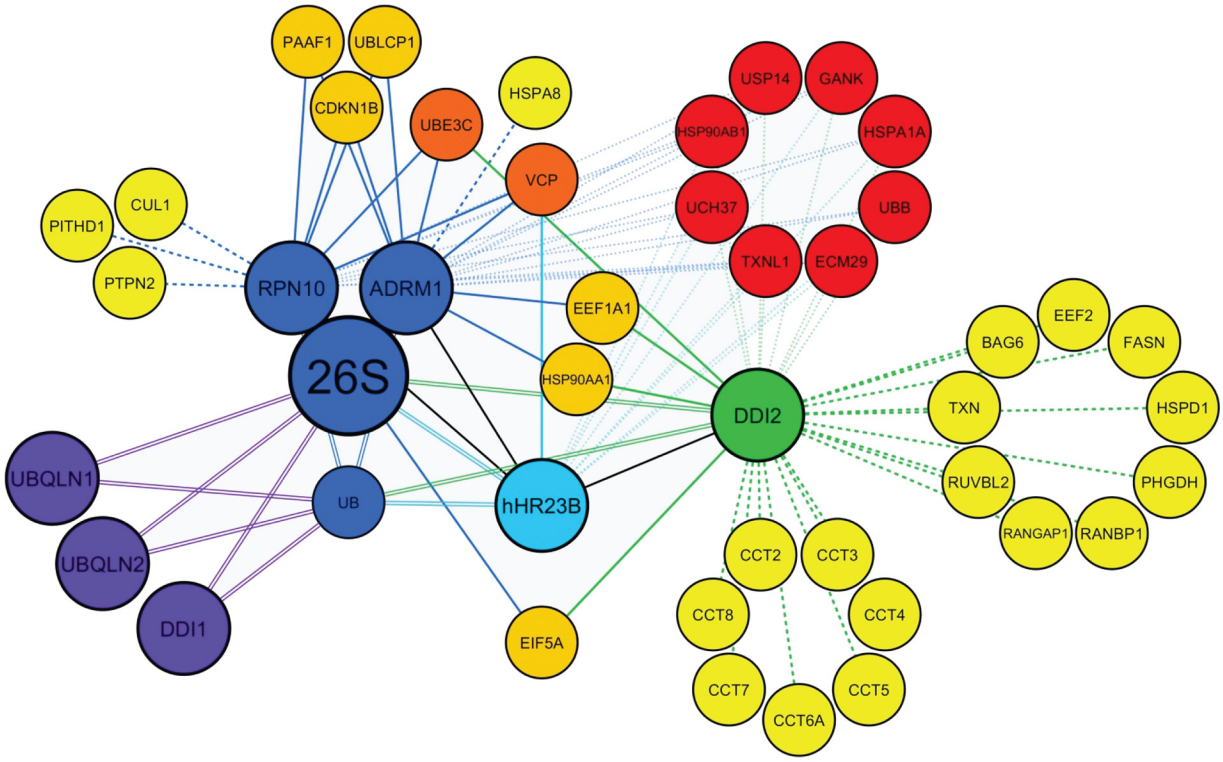

FIG. 6. **Protein interaction topologies of the seven UbR-proteasome complexes.** Smaller nodes (yellow, orange, red) represent prey whereas larger nodes (green, blue, cyan, violet) represent baits. Edges between nodes represent capture of prey by bait, designated by the color of the edge. Black edges denote reciprocal capture by preys to one another, whereas edge types denote the number of baits that captured each prey, *i.e.* 1-dashed, 2 or 3-solid, 4-dotted, and 7-parallel.

interaction and connectivity are illustrated in Fig. 6. Among these PIPs, ubiquitin was the only protein captured by all baits, further validating that all UbRs are involved in recognizing ubiquitinated substrates. In addition to ubiquitin, seven unique PIPs (*i.e.* Usp14, Uch37, Ecm29, Gankyrin/p28, Hsp90/Hsp90AB1, Hsp70/HSPA1A, Txnl1) were all identified in AR, RR, BR and D2R samples. Although hHR23B is the bait for the BR sample, it was also identified in AR, RR and D2R samples indicating non-overlapping engagement with the proteasome. In comparison, Ddi2 was only found in BR samples, suggesting that hHR23B and Ddi2 may interact closely in cells. All of these PIPs have good correlation in abundance among the samples (Fig. 4), similar to those of proteasome subunits, implying that they associate with core proteasomes similarly in UbR-proteasome subcomplexes and are key PIPs involved in proteasomal degradation. In addition, although one PIP (*i.e.* UBE3C) was shared by AR, RR, and D2R samples, another PIP (*i.e.* p97/VCP) was shared by AR, RR and BR samples. Moreover, three PIPs (*i.e.* p27, PAAF1, UBLCP1) were only identified in AR and RR samples, indicating that these proteins interact with specific subgroups of proteasome complexes. It is noted that 16 unique putative PIPs were identified only in D2R samples, including seven subunits of the 8-member CCT complex. The CCT complex was previously identified as PIPs using the QTAX strategy (48), and functions as a molecular chaperone to assist the folding of proteins upon ATP hydrolysis. Interestingly, the stability of the CCT complex was previously shown to be dependent on proteasomal degradation (62). Our results suggest that Ddi2 may be the physical link between the CCT complex and the proteasome for the degradation of its own constituents or associated substrates. Given the number of interactions present in the Ddi2-proteasome complex, it warrants further investigation to determine the role of Ddi2 during proteasomal degradation. Collectively, although UbR-proteasome complexes possess the same core 26S proteasome and share a few PIPs, they do have unique protein interactions that may link them to specific cellular pathways through their roles in proteasomal degradation.

DISCUSSION

Protein complexes, such as proteasomes, exist in cells as dynamic and heterogeneous entities, often comprising multiple subcomplexes responsible for various functions. Effective isolation of these dynamic subcomplexes is a prerequisite to detailed proteomic analysis for understanding their structural and functional similarities and differences. In this work, we report a new method, XBAP, and applied it to efficient capture and purification of dynamic proteasome subcomplexes containing ubiquitin receptors. The XBAP strategy enables the stabilization of dynamic protein interactions through limited *in vivo* cross-linking. In comparison to our previously developed QTAX strategy (47), XBAP utilizes a significantly lower amount of formaldehyde ($\leq$ 0.05% *versus* 1%) for *in vivo* cross-linking. Our results have shown that low level FA *in vivo* cross-linking helps to maintain the intactness of the 26S proteasome complexes under physiological conditions. This is based on the observation that proteasomal activities were increased when comparing cross-linked and uncross-linked lysates. This finding suggests that the interaction of proteasome complexes is prone to change during native cell lysis. Indeed, FA cross-linking not only better maintains the intactness of the 26S holocomplex, but also enables consistent capture of proteasome components as well as dynamic and weak interactors of proteasomes. For example, the interaction of proteasome regulator Ecm29 with the proteasome is labile and susceptible to change under native conditions (63). Because of this, Ecm29 is often missed in purified mammalian proteasomes (45, 46). Here, we have reproducibly captured Ecm29 after FA cross-linking, which corroborates well with previous results (48, 54). In addition, dynamic proteasome interactors have displayed much higher abundances in isolated proteasome complexes after cross-linking when comparing to noncross-linked samples. Together, our results demonstrate that mild FA cross-linking is beneficial for native purifications through preservation of protein interactions without sacrificing the integrity and functionality of protein complexes. In addition, limited FA cross-linking does not interfere with native cell lysis, subsequent purification and mass spectrometric analysis. Moreover, it minimizes the impact of cell lysis on protein interactions under native conditions and eliminates purification background. Clearly, the level of *in vivo* FA cross-linking can be modulated to fit the needs of all types of purification procedures regardless of lysis conditions, thus expanding the scope of interactions for investigation.

Another unique feature of the XBAP strategy is the utilization of HF and TB tags for the two selected baits, permitting bimolecular purification not only under native conditions, but also QTAX-type of experiments under fully denaturing conditions (47). This advantage is because of the fact that Histidine and Biotin tags are the only two tags that can tolerate fully denaturing conditions (44). Such flexibility would be advantageous when experiments require the maximum elimination of any reorganization of protein interactions during cell lysis and nonspecific interactions during purification. Additionally, when sufficient cross-linking is required for capturing protein interactions of all natures including weak/transient ones and for identifying protein interaction interfaces in living cells, denaturing purification would be ideal (47–49). Importantly, the employment of two tagged baits enables the dissection of heterogeneous protein complexes into subpopulations. Such dual-tagged cell lines also permit enhanced identification of protein-protein interaction contact sites in selectively enriched subcomplexes using cross-linking mass spectrometry (49). Specifically, future studies are warranted to employ $293^{\text{HF-UbR\_Rpn11-TB}}$ cells generated in this work to determine how each UbR docks on proteasomes in living cells, thus uncovering molecular details underlying how UbRs deliver

substrates to proteasomes. Collectively, the development of the XBAP strategy augments our ability to define dynamic protein complexes in more detail, and this strategy can be applied to study other protein complexes.

With the XBAP strategy, we have effectively identified seven UbR-proteasome subcomplexes and quantitatively compared their subunit compositions and relative abundance based on label-free quantitative mass spectrometry using MaxQuant (55, 56). Correlation analysis has revealed that all of these UbR-proteasome complexes contain the same type of core 26S proteasome holocomplex in regards to its composition and stoichiometry. Among the selected UbRs, Rpn10 and Rpn13/ADRM1 are inherent subunits of the 26S holocomplex, and expected to possess the same core proteasome subunits that assemble into the functional entity. The fact that all of the selected UbRs bind to the same proteasome entity as Rpn13/ADRM1 and Rpn10, further validates that UbRs transport polyubiquitinated substrates to the same population of proteasomes for degradation. Although the stoichiometry of proteasome subunits remains similar in UbR-proteasome complexes, there are differences in the amount of UbRs associating with proteasomes. In addition to essential proteasome subunits, Rpn13/ADRM1 and Rpn10 have copurified three 20S activator proteins PA28α, PA28γ, and PA200, suggesting the presence of hybrid 26S proteasomes. However, these activator proteins are very low in abundance compared with other 19S subunits. In addition, non-proteasome UbRs did not capture these activators. Previous reports have suggested that the most abundant activator bound to the 20S core complex is the 19S RP in mammalian cells (38). Together, these results confirm that the 26S holocomplex is the main machinery responsible for the degradation of ubiquitinated substrates.

Apart from proteasome subunits, K48-linked ubiquitin chains, the common ubiquitin signal for proteasomal degradation (2, 64), have been identified in all XBAP-MS experiments. However, this finding does not exclude the involvement of other ubiquitin linkages in targeting proteins to proteasomes for degradation. To fully dissect the ubiquitin topologies bound to UbR-proteasomes, proteasome inhibition will be needed to prevent the degradation of less abundant ubiquitin signals. In addition, the XBAP strategy can be altered to study UbR-bound ubiquitin by tagging a UbR and Ub respectively, which would help uncover ubiquitin signals recognized by UbRs for proteasomal degradation.

During XBAP experiments, UbRs were used as the first bait, and Rpn11 was used as the second bait. The resulting complexes would contain proteins that interact with both of these baits. Although UbR interacting proteins may be purified and identified using UbRs as single baits, most of them are not expected to be present in UbR-proteasome complexes if they only interact with UbRs. In addition, sequential purification using two different baits can lead to the loss of low abundant protein interactors. Nonetheless, a total of 38 putative PIPs were identified from AR, RR, BR, and D2R samples. Among them, seven known PIPs (*i.e.* Uch37, Usp14/Ubp6, Ecm29, Gankyrin/p28, Hsp90/HSP90AB1, Hsp70/HSPA1A, and Txnl1) were identified in all of the four samples, all of which are key regulators of proteasomal degradation (7, 8). For example, Uch37 and Usp14/Ubp6 are two deubiquitinating enzymes that dynamically interact with the 26S proteasome with fast on/off rates (46) and have not been consistently identified in proteasomes isolated under native conditions. They function to trim the polyubiquitin chains on delivered substrates at the proteasome (8, 65–68). In contrast to intrinsic proteasome deubiquitinase Rpn11 which promotes degradation, Uch37 and Usp14/Ubp6 appear to antagonize the degradation of ubiquitinated substrates (67, 69), suggesting that they are important for recycling ubiquitin and maintaining ubiquitin levels in cells. Although Uch37 interacts with the proteasome through Rpn13/ADRM1 (65, 70, 71), Usp14/Ubp6 physically binds to proteasome subunit Rpn1 (30, 60, 72), and interacts with Rpt1 when conjugated to a ubiquitin aldehyde (73, 74). The presence of Uch37 and Usp14/Ubp6 in UbR-proteasome complexes further indicate that these deubiquitinases are major players in regulating substrate processing at the proteasome.

Another well-recognized proteasome regulator is Ecm29, which has been suggested to modulate the interaction between the 20S and 19S complexes and inhibit proteasome functions (75, 76). However, under oxidative stress, Ecm29 is enriched at the 19S proteasome and is responsible for triggering the disassembly of the 26S holocomplex, leading to increased ubiquitin and ATP-independent degradation of oxidized proteins to maintain cell homeostasis (63). In addition, Ecm29 can link the 26S proteasome to specific cellular compartments through its interactions with molecular motors and endosomal components (77), and to Toll-like receptor 3 (TLR3) signaling through the effect of Ecm29 on the levels of TLR3 and proteins involved in autophagy (78). Although Ecm29 is involved in multiple cellular pathways through its action on the assembly and function of proteasomes, it has been challenging to purify Ecm29 with proteasomes without *in vivo* cross-linking. Given the diverse biological roles of Ecm29, the difficulty of capturing its interaction with proteasomes, and its existence in multiple UbR-proteasome complexes, we speculate that the population of Ecm29-containing proteasomes may be much more abundant in cells than previously expected. With the development of XBAP, the function of Ecm29 in regulating proteasomes can be further investigated through detailed characterization of Ecm29-proteasome subcomplexes under different physiology conditions.

The assembly of the 19S RP is assisted by four chaperons (79), three of which (*i.e.* Gankyrin/p28, p27, PAAF1) have been identified in this work. Although Gankyrin/p28 was present in AR, RR, BR, and D2R samples, p27 and PAAF1 were only observed in AR and RR samples. During the initial step of the base subcomplex assembly, Gankyrin/p28 and PAAF1 asso-

ciate with Rpt3-Rpt6 to build an intermediate module, whereas p27 forms a modulator trimer complex with Rpt4 and Rpt5 (80). As both Rpn13/ADRM1 and Rpn10 are components of the 19S RP assembly, it is not surprising that these RP chaperons can be found in Rpn13/ADRM1- and Rpn10-containing proteasome complexes. This implies that subassemblies may be co-purified; however, their relative abundances are much lower than mature proteasomes. In comparison, Gankyrin/p28 was found not only in AR and RR samples, but also in BR and D2R samples, and has higher abundances than p27 and PAAF1 in the UbR-proteasome complexes (Supplemental Table 1). Currently Gankyrin/p28 has been considered as an oncogene involved in tumorigenesis by promoting the degradation of Rb and p53 (8). Together, it is reasonable to suspect that the frequent occurrence of Gankyrin/p28 at various UbR-proteasome complexes may be attributed to its additional functions aside from its role as a RP chaperon.

Among the seven PIPs shared by AR, RR, BR and D2R sample, two ATP-dependent chaperons Hsp70 and Hsp90 were also identified. Both are known to regulate *de novo* and stress-related protein folding and stability (81). These proteins have been previously identified as PIPs (46–48, 82), and their involvement in mediating proteasomal degradation is thought to be partially because of their interactions with the co-chaperon CHIP which functions as an E3 ubiquitin ligase using a modified RING finger domain (U-box) (81). In addition, Hsp70 has been shown to bind to the 19S RP and play a role in modulating the 26S proteasome disassembly upon oxidative stress (82). Interestingly, Hsp90 has also been suggested to be important in the ATP-dependent assembly and maintenance of the 26S proteasome (83). Moreover, Hsp90 has been linked to proteasomes through its interaction with p97/VCP (Transitional endoplasmic reticulum ATPase) (84), a key component in mediating ubiquitination and degradation of misfolded proteins through ER-associated degradation pathway (ERAD). Interestingly, p97/VCP interacts with hHR23B and has been identified in AR, RR and BR samples. Although hHR23B is one of the two baits for BR samples, it has also been co-purified in AR, RR and D2R samples. In addition, the amount of hHR23B-associated proteasomes is very similar that of Rpn10-bound proteasomes. Together, this implies that hHR23B is one of the major components of the 26S proteasome, and the most abundant non-proteasome UbR at the proteasome. This corroborates well with previous reports that hHR23B has been more frequently identified in proteasomes in both yeast and mammalian cells (46, 47). In addition to its role in delivering polyubiquitinated substrates, hHR23B may be responsible for linking other players such as Hsp90 and VCP-containing chaperon complexes to proteasomes. It has been suggested that non-proteasome UbRs may interact in cells because of the presence of UBA and UBL domains (85). In this work, we have confidently identified the interaction between hHR23B and Ddi2 when using either one as the bait, suggesting that these two non-proteasome UbRs may cooperate in shuttling ubiquitinated substrates.

Another protein found in all of AR, RR, BR and D2R samples is Txnl1 (thioredoxin-like protein 1), which exhibits thioredoxin activity in cells. It has been shown that Txnl1 binds to Rpn11 and targets eEF1A1 *in vivo* (86), thus linking protein reduction and degradation pathways. eEF1A1, a known PIP, is thought to specifically interact with Rpt1 (87), and is involved in transferring misfolded nascent proteins from the ribosome to the 26S proteasome for degradation (87). Although Rad23 and Rpn10 are suspected to be involved in the degradation of damaged proteins (87), eEF1A1 was detected only in AR and D2R samples, suggesting that eEF1A1 may be more associated with Rpn13/ADRM1- and Ddi2-proteasome subcomplexes.

In contrast to AR, RR, BR and D2R samples, it is noted that U1R, U2R and D1R samples did not identify any PIPs except core proteasome subunits and ubiquitin. Even though the expression levels of Ubqln1, Ubqln2 and Ddi1 are similar to other UbRs (Fig. 1), the amount of proteasomes associated with Ubqln1, Ubqln2 and Ddi1 are apparently much lower based on spectral counts (Supplemental Table 1). We note that we did not detect known interactors of Ubqln1 and Ubqln2 such as Hsp70 or p97/VCP (88, 89). XBAP experiments selectively purify proteins that are bound to proteasomes complexed with UbRs and cannot identify proteins that specifically interact with either Rpn11 or UbR. These known interactors may thus not be part of a stable higher order complex, or interactions may be below our detection limit. To enhance the detection of proteins known to interact with both UbRs and proteasomes, one possibility is to increase the interaction between UbRs and proteasomes through proteasome inhibition. This may also improve the identification of potential proteasomal substrates recognized and delivered by these UbRs.

Very recently, two proteasome subunits Dss1/Rpn15 and Rpn1 have been identified as novel types of ubiquitin receptors in yeast (30, 90). Dss1/Rpn15 is an intrinsically disordered protein and does not contain any known ubiquitin binding domains. Instead, its interaction with ubiquitin is mediated through various acidic and hydrophobic residues. Surprisingly, the ubiquitin binding region of Dss1/Rpn15 overlaps with its proteasome binding site, and a recent study has questioned its authenticity as a UbR (30). In comparison, the Rpn1 toroid possesses two unique binding domains, T1 (toroid 1) and T2 (toroid 2) (30). Although T2 binds to UBL deubiquitinase Usp14/Ubp6, T1 functions to recruit substrates directly by binding to ubiquitin itself and indirectly by binding to UBL shuttling factors, a feature shared by Rpn10 and Rpn13/ADRM1 despite a lack of structural similarity among these receptors (30). Clearly, the XBAP strategy can be applied to dissect structural and functional diversities of these new UbR containing protein complexes in future studies

and thus understand their roles in the UPS and other cellular pathways.

In summary, we have developed a new integrated strategy to effectively isolate dynamic UbR-proteasome complexes for proteomic analysis and characterization. Importantly, the XBAP strategy can be directly adopted to decipher the structural and compositional heterogeneity of other protein complexes. When coupled with newly developed cross-linking reagents (49, 91), the XBAP method can be employed to determine protein interaction interfaces of protein complexes using cross-linking mass spectrometry. In addition, such a strategy can be extended to determine whether and how proteins form homo- or hetero-dimers in living cells. Collectively, the methodology presented here provides a solid basis to further advance the studies of protein complexes by proteomic approaches.

Acknowledgments—We thank Drs. A.L. Burlingame and Robert Chalkley for the developmental version of Protein Prospector. We thank Dr. Mervyn J. Monteiro at University of Maryland for Ubqln1 plasmids.

* This work was supported by National Institutes of Health grants RO1GM074830 to L.H, R01GM106003 to L.H. and S. R., R01GM066164 and R01GM066164-S1 to P.K., and by Intramural Research Program of the NIH, National Cancer Institute, Center for Cancer Research to K.J.W. The content is solely the responsibility of the authors and does not necessarily represent the official views of the National Institutes of Health.

S This article contains supplemental material.

** To whom correspondence should be addressed: Medical Science I, D233, Department of Physiology & Biophysics, University of California, Irvine, Irvine, CA 92697–4560. Tel.: 949-824 8548; Fax: 949-824 8540; E-mail: lanhuang@uci.edu.

‡‡ These authors contributed equally to this work.

REFERENCES

1. Pickart, C. M., and Cohen, R. E. (2004) Proteasomes and their kin: proteases in the machine age. *Nat. Rev. Mol. Cell Biol.* **5**, 177–187
2. Finley, D. (2009) Recognition and processing of ubiquitin-protein conjugates by the proteasome. *Annu. Rev. Biochem.* **78,** 477–513
3. Finley, D., Chen, X., and Walters, K. J. (2015) Gates, Channels, and Switches: Elements of the Proteasome Machine. *Trends Biochem Sci.* **41,** 77–93
4. Löwe, J., Stock, D., Jap, B., Zwickl, P., Baumeister, W., and Huber, R. (1995) Crystal structure of the 20S proteasome from the archaeon T. acidophilum at 3.4 Å resolution. *Science* **268,** 533–539
5. Groll, M., Ditzel, L., Löwe, J., Stock, D., Bochtler, M., Bartunik, H. D., and Huber, R. (1997) Structure of 20S proteasome from yeast at 2.4 A resolution. *Nature* **386,** 463–471
6. Glickman, M. H., Rubin, D. M., Fried, V. A., and Finley, D. (1998) The regulatory particle of the Saccharomyces cerevisiae proteasome. *Mol. Cell. Biol.* **18,** 3149–3162
7. Schmidt, M., Hanna, J., Elsasser, S., and Finley, D. (2005) Proteasome-associated proteins: regulation of a proteolytic machine. *Biol. Chem.* **386,** 725–737
8. Schmidt, M., and Finley, D. (2014) Regulation of proteasome activity in health and disease. *Biochim. Biophys. Acta* **1843,** 13–25
9. Beck, F., Unverdorben, P., Bohn, S., Schweitzer, A., Pfeifer, G., Sakata, E., Nickell, S., Plitzko, J.M., Villa, E., Baumeister, W., and Forster, F. (2012) Near-atomic resolution structural model of the yeast 26S proteasome. *Proc. Natl. Acad. Sci. U S A* **109,** 14870–14875
10. Lander, G. C., Estrin, E., Matyskiela, M. E., Bashore, C., Nogales, E., and Martin, A. (2012) Complete subunit architecture of the proteasome regulatory particle. *Nature* **482,** 186–191
11. Lasker, K., Forster, F., Bohn, S., Walzthoeni, T., Villa, E., Unverdorben, P., Beck, F., Aebersold, R., Sali, A., and Baumeister, W. (2012) Molecular architecture of the 26S proteasome holocomplex determined by an integrative approach. *Proc. Natl. Acad. Sci. U S A* **109,** 1380–1387
12. Di Fiore, P. P., Polo, S., and Hofmann, K. (2003) When ubiquitin meets ubiquitin receptors: a signalling connection. *Nat. Rev. Mol. Cell Biol.* **4,** 491–497
13. van Nocker, S., Sadis, S., Rubin, D. M., Glickman, M., Fu, H., Coux, O., Wefes, I., Finley, D., and Vierstra, R. D. (1996) The multiubiquitin-chain-binding protein Mcb1 is a component of the 26S proteasome in Saccharomyces cerevisiae and plays a nonessential, substrate-specific role in protein turnover. *Mol. Cell Biol.* **16,** 6020–6028
14. Husnjak, K., Elsasser, S., Zhang, N., Chen, X., Randles, L., Shi, Y., Hofmann, K., Walters, K. J., Finley, D., and Dikic, I. (2008) Proteasome subunit Rpn13 is a novel ubiquitin receptor. *Nature* **453,** 481–488
15. Marin, I. (2014) The ubiquilin gene family: evolutionary patterns and functional insights. *BMC Evol. Biol.* **14,** 63
16. Elsasser, S., and Finley, D. (2005) Delivery of ubiquitinated substrates to protein-unfolding machines. *Nat. Cell Biol.* **7,** 742–749
17. Chen, L., and Madura, K. (2006) Evidence for distinct functions for human DNA repair factors hHR23A and hHR23B. *FEBS Lett.* **580,** 3401–3408
18. Pilarsky, C., Wenzig, M., Specht, T., Saeger, H. D., and Grutzmann, R. (2004) Identification and validation of commonly overexpressed genes in solid tumors by comparison of microarray data. *Neoplasia* **6,** 744–750
19. Fejzo, M. S., Anderson, L., von Euw, E. M., Kalous, O., Avliyakulov, N. K., Haykinson, M. J., Konecny, G. E., Finn, R. S., and Slamon, D. J. (2013) Amplification Target ADRM1: Role as an Oncogene and Therapeutic Target for Ovarian Cancer. *Int. J. Mol. Sci.* **14,** 3094–3109
20. Anchoori, R. K., Karanam, B., Peng, S., Wang, J. W., Jiang, R., Tanno, T., Orlowski, R. Z., Matsui, W., Zhao, M., Rudek, M. A., Hung, C. F., Chen, X., Walters, K. J., and Roden, R. B. (2013) A bis-benzylidine piperidone targeting proteasome ubiquitin receptor RPN13/ADRM1 as a therapy for cancer. *Cancer Cell* **24,** 791–805
21. Trader, D. J., Simanski, S., and Kodadek, T. (2015) A reversible and highly selective inhibitor of the proteasomal ubiquitin receptor rpn13 is toxic to multiple myeloma cells. *J. Am. Chem. Soc.* **137,** 6312–6319
22. Fotheringham, S., Epping, M. T., Stimson, L., Khan, O., Wood, V., Pezzella, F., Bernards, R., and La Thangue, N. B. (2009) Genome-wide loss-of-function screen reveals an important role for the proteasome in HDAC inhibitor-induced apoptosis. *Cancer Cell* **15,** 57–66
23. Khan, O., Fotheringham, S., Wood, V., Stimson, L., Zhang, C., Pezzella, F., Duvic, M., Kerr, D. J., and La Thangue, N. B. (2010) HR23B is a biomarker for tumor sensitivity to HDAC inhibitor-based therapy. *Proc. Natl. Acad. Sci. U S A* **107,** 6532–6537
24. Kang, Y., Chen, X., Lary, J. W., Cole, J. L., and Walters, K. J. (2007) Defining how ubiquitin receptors hHR23a and S5a bind polyubiquitin. *J. Mol. Biol.* **369,** 168–176
25. Schreiner, P., Chen, X., Husnjak, K., Randles, L., Zhang, N., Elsasser, S., Finley, D., Dikic, I., Walters, K. J., and Groll, M. (2008) Ubiquitin docking at the proteasome through a novel pleckstrin-homology domain interaction. *Nature* **453,** 548–552
26. Matyskiela, M. E., Lander, G. C., and Martin, A. (2013) Conformational switching of the 26S proteasome enables substrate degradation. *Nat. Struct. Mol. Biol.* **20,** 781–788
27. Lu, X., Liu, F., Durham, S. E., Tarasov, S. G., and Walters, K. J. (2015) A High Affinity hRpn2-Derived Peptide That Displaces Human Rpn13 from Proteasome in 293T Cells. *PLoS One* **10,** e0140518
28. Ito, T., Chiba, T., Ozawa, R., Yoshida, M., Hattori, M., and Sakaki, Y. (2001) A comprehensive two-hybrid analysis to explore the yeast protein interactome. *Proc. Natl. Acad. Sci. U.S.A.* **98,** 4569–4574
29. Elsasser, S., Gali, R. R., Schwickart, M., Larsen, C. N., Leggett, D. S., Muller, B., Feng, M. T., Tubing, F., Dittmar, G. A., and Finley, D. (2002) Proteasome subunit Rpn1 binds ubiquitin-like protein domains. *Nat. Cell Biol.* **4,** 725–730
30. Shi, Y., Chen, X., Elsasser, S., Stocks, B. B., Tian, G., Lee, B. H., Zhang, N., de Poot, S. A., Tuebing, F., Sun, S., Vannoy, J., Tarasov, S. G., Engen, J. R., Finley, D., and Walters, K.J. (2016) Rpn1 provides adjacent receptor sites for substrate binding and deubiquitination by the proteasome. *Science* **351** (6275) pii: aad9421
31. Hiyama, H., Yokoi, M., Masutani, C., Sugasawa, K., Maekawa, T., Tanaka,

K., Hoeijmakers, J. H., and Hanaoka, F. (1999) Interaction of hHR23 with S5a. The ubiquitin-like domain of hHR23 mediates interaction with S5a subunit of 26 S proteasome. *J. Biol. Chem.* **274,** 28019–28025
32. Walters, K. J., Kleijnen, M. F., Goh, A. M., Wagner, G., and Howley, P. M. (2002) Structural studies of the interaction between ubiquitin family proteins and proteasome subunit S5a. *Biochemistry* **41,** 1767–1777
33. Ko, H. S., Uehara, T., Tsuruma, K., and Nomura, Y. (2004) Ubiquilin interacts with ubiquitylated proteins and proteasome through its ubiquitin-associated and ubiquitin-like domains. *FEBS Lett.* **566,** 110–114
34. Elsasser, S., Chandler-Militello, D., Muller, B., Hanna, J., and Finley, D. (2004) Rad23 and Rpn10 serve as alternative ubiquitin receptors for the proteasome. *J. Biol. Chem.* **279,** 26817–26822
35. Verma, R., Oania, R., Graumann, J., and Deshaies, R. J. (2004) Multiubiquitin chain receptors define a layer of substrate selectivity in the ubiquitin-proteasome system. *Cell* **118,** 99–110
36. Huang, L., and Burlingame, A. L. (2005) Comprehensive mass spectrometric analysis of the 20S proteasome complex. *Methods Enzymol.* **405,** 187–236
37. Drews, O., Wildgruber, R., Zong, C., Sukop, U., Nissum, M., Weber, G., Gomes, A. V., and Ping, P. (2007) Mammalian proteasome subpopulations with distinct molecular compositions and proteolytic activities. *Mol. Cell Proteomics* **6,** 2021–2031
38. Fabre, B., Lambour, T., Garrigues, L., Ducoux-Petit, M., Amalric, F., Monsarrat, B., Burlet-Schiltz, O., and Bousquet-Dubouch, M. P. (2014) Label-free quantitative proteomics reveals the dynamics of proteasome complexes composition and stoichiometry in a wide range of human cell lines. *J. Proteome Res.* **13,** 3027–3037
39. Gavin, A. C., Aloy, P., Grandi, P., Krause, R., Boesche, M., Marzioch, M., Rau, C., Jensen, L. J., Bastuck, S., Dumpelfeld, B., Edelmann, A., Heurtier, M. A., Hoffman, V., Hoefert, C., Klein, K., Hudak, M., Michon, A. M., Schelder, M., Schirle, M., Remor, M., Rudi, T., Hooper, S., Bauer, A., Bouwmeester, T., Casari, G., Drewes, G., Neubauer, G., Rick, J. M., Kuster, B., Bork, P., Russell, R. B., and Superti-Furga, G. (2006) Proteome survey reveals modularity of the yeast cell machinery. *Nature* **440,** 631–636
40. Krogan, N. J., Cagney, G., Yu, H., Zhong, G., Guo, X., Ignatchenko, A., Li, J., Pu, S., Datta, N., Tikuisis, A. P., Punna, T., Peregrin-Alvarez, J. M., Shales, M., Zhang, X., Davey, M., Robinson, M. D., Paccanaro, A., Bray, J. E., Sheung, A., Beattie, B., Richards, D. P., Canadien, V., Lalev, A., Mena, F., Wong, P., Starostine, A., Canete, M. M., Vlasblom, J., Wu, S., Orsi, C., Collins, S. R., Chandran, S., Haw, R., Rilstone, J. J., Gandi, K., Thompson, N. J., Musso, G., St Onge, P., Ghanny, S., Lam, M. H., Butland, G., Altaf-Ul, A. M., Kanaya, S., Shilatifard, A., O'Shea, E., Weissman, J. S., Ingles, C. J., Hughes, T. R., Parkinson, J., Gerstein, M., Wodak, S.J., Emili, A., and Greenblatt, J. F. (2006) Global landscape of protein complexes in the yeast Saccharomyces cerevisiae. *Nature* **440,** 637–643
41. Collins, S. R., Kemmeren, P., Zhao, X. C., Greenblatt, J. F., Spencer, F., Holstege, F. C., Weissman, J. S., and Krogan, N. J. (2007) Toward a comprehensive atlas of the physical interactome of Saccharomyces cerevisiae. *Mol. Cell. Proteomics* **6,** 439–450
42. Herzog, F., Kahraman, A., Boehringer, D., Mak, R., Bracher, A., Walzthoeni, T., Leitner, A., Beck, M., Hartl, F. U., Ban, N., Malmstrom, L., and Aebersold, R. (2012) Structural probing of a protein phosphatase 2A network by chemical cross-linking and mass spectrometry. *Science* **337,** 1348–1352
43. Starokadomskyy, P., and Burstein, E. (2014) Bimolecular affinity purification: a variation of TAP with multiple applications. *Methods Mol. Biol.* **1177,** 193–209
44. Tagwerker, C., Flick, K., Cui, M., Guerrero, C., Dou, Y., Auer, B., Baldi, P., Huang, L., and Kaiser, P. (2006) A tandem affinity tag for two-step purification under fully denaturing conditions: application in ubiquitin profiling and protein complex identification combined with in vivocross-linking. *Mol. Cell. Proteomics.* **5,** 737–748
45. Wang, X., Chen, C. F., Baker, P. R., Chen, P. L., Kaiser, P., and Huang, L. (2007) Mass spectrometric characterization of the affinity-purified human 26S proteasome complex. *Biochemistry* **46,** 3553–3565
46. Wang, X., and Huang, L. (2008) Identifying dynamic interactors of protein complexes by quantitative mass spectrometry. *Mol. Cell. Proteomics* **7,** 46–57
47. Guerrero, C., Tagwerker, C., Kaiser, P., and Huang, L. (2006) An integrated mass spectrometry-based proteomic approach: quantitative analysis of tandem affinity-purified in vivo cross-linked protein complexes (QTAX) to decipher the 26 S proteasome-interacting network. *Mol. Cell. Proteomics* **5,** 366–378
48. Guerrero, C., Milenkovic, T., Przulj, N., Kaiser, P., and Huang, L. (2008) Characterization of the proteasome interaction network using a QTAX-based tag-team strategy and protein interaction network analysis. *Proc. Natl. Acad. Sci. U S A* **105,** 13333–13338
49. Kaake, R. M., Wang, X., Burke, A., Yu, C., Kandur, W., Yang, Y., Novtisky, E. J., Second, T., Duan, J., Kao, A., Guan, S., Vellucci, D., Rychnovsky, S. D., and Huang, L. (2014) A new in vivo cross-linking mass spectrometry platform to define protein-protein interactions in living cells. *Mol. Cell. Proteomics* **13,** 3533–3543
50. Kaake, R. M., Milenkovic, T., Przulj, N., Kaiser, P., and Huang, L. (2010) Characterization of cell cycle specific protein interaction networks of the yeast 26S proteasome complex by the QTAX strategy. *J. Proteome Res.* **9,** 2016–2029
51. Fang, L., Kaake, R. M., Patel, V. R., Yang, Y., Baldi, P., and Huang, L. (2012) Mapping the protein interaction network of the human COP9 signalosome complex using a label-free QTAX strategy. *Mol. Cell Proteomics* **11,** 138–147
52. Subbotin, R. I., and Chait, B. T. (2014) A pipeline for determining protein-protein interactions and proximities in the cellular milieu. *Mol. Cell. Proteomics.* **13,** 2824–2835
53. Smart, S. K., Mackintosh, S. G., Edmondson, R. D., Taverna, S. D., and Tackett, A. J. (2009) Mapping the local protein interactome of the NuA3 histone acetyltransferase. *Protein Sci.* **18,** 1987–1997
54. Fabre, B., Lambour, T., Delobel, J., Amalric, F., Monsarrat, B., Burlet-Schiltz, O., and Bousquet-Dubouch, M.P. (2013) Subcellular distribution and dynamics of active proteasome complexes unraveled by a workflow combining in vivo complex cross-linking and quantitative proteomics. *Mol. Cell. Proteomics.* **12,** 687–699
55. Cox, J., and Mann, M. (2008) MaxQuant enables high peptide identification rates, individualized p.p.b.-range mass accuracies and proteome-wide protein quantification. *Nat. Biotechnol.* **26,** 1367–1372
56. Cox, J., Hein, M. Y., Luber, C. A., Paron, I., Nagaraj, N., and Mann, M. (2014) Accurate proteome-wide label-free quantification by delayed normalization and maximal peptide ratio extraction, termed MaxLFQ. *Mol. Cell. Proteomics* **13,** 2513–2526
57. Deng, H. X., Chen, W., Hong, S. T., Boycott, K. M., Gorrie, G. H., Siddique, N., Yang, Y., Fecto, F., Shi, Y., Zhai, H., Jiang, H., Hirano, M., Rampersaud, E., Jansen, G. H., Donkervoort, S., Bigio, E. H., Brooks, B. R., Ajroud, K., Sufit, R. L., Haines, J. L., Mugnaini, E., Pericak-Vance, M. A., and Siddique, T. (2011) Mutations in UBQLN2 cause dominant X-linked juvenile and adult-onset ALS and ALS/dementia. *Nature* **477,** 211–215
58. El Ayadi, A., Stieren, E. S., Barral, J. M., and Boehning, D. (2013) Ubiquilin-1 and protein quality control in Alzheimer disease. *Prion* **7,** 164–169
59. Verma, R., Aravind, L., Oania, R., McDonald, W. H., Yates, J. R. I., Koonin, E. V., and Deshaies, R. J. (2002) Role of Rpn11 metalloprotease in deubiquitination and degradation by the 26S proteasome. *Science* **298,** 611–615
60. Leggett, D. S., Hanna, J., Borodovsky, A., Crosas, B., Schmidt, M., Baker, R. T., Walz, T., Ploegh, H., and Finley, D. (2002) Multiple associated proteins regulate proteasome structure and function. *Mol. Cell* **10,** 495–507
61. Berko, D., Herkon, O., Braunstein, I., Isakov, E., David, Y., Ziv, T., Navon, A., and Stanhill, A. (2014) Inherent asymmetry in the 26S proteasome is defined by the ubiquitin receptor RPN13. *J. Biol. Chem.* **289,** 5609–5618
62. Yokota, S., Kayano, T., Ohta, T., Kurimoto, M., Yanagi, H., Yura, T., and Kubota, H. (2000) Proteasome-dependent degradation of cytosolic chaperonin CCT. *Biochem. Biophys. Res. Commun.* **279,** 712–717
63. Wang, X., Yen, J., Kaiser, P., and Huang, L. (2010) Regulation of the 26S proteasome complex during oxidative stress. *Sci. Signal.* **3,** ra88
64. Ciechanover, A., and Stanhill, A. (2014) The complexity of recognition of ubiquitinated substrates by the 26S proteasome. *Biochim. Biophys. Acta* **1843,** 86–96
65. Yao, T., Song, L., Xu, W., DeMartino, G. N., Florens, L., Swanson, S. K., Washburn, M. P., Conaway, R. C., Conaway, J. W., and Cohen, R. E. (2006) Proteasome recruitment and activation of the Uch37 deubiquitinating enzyme by Adrm1. *Nat. Cell Biol.* **8,** 994–1002
66. Koulich, E., Li, X., and DeMartino, G. N. (2008) Relative structural and functional roles of multiple deubiquitylating proteins associated with

mammalian 26S proteasome. *Mol. Biol. Cell* **19,** 1072–1082
67. Hanna, J., Hathaway, N. A., Tone, Y., Crosas, B., Elsasser, S., Kirkpatrick, D. S., Leggett, D. S., Gygi, S. P., King, R. W., and Finley, D. (2006) Deubiquitinating enzyme Ubp6 functions noncatalytically to delay proteasomal degradation. *Cell* **127,** 99–111
68. Lee, B. H., Lee, M. J., Park, S., Oh, D. C., Elsasser, S., Chen, P. C., Gartner, C., Dimova, N., Hanna, J., Gygi, S. P., Wilson, S. M., King, R. W., and Finley, D. (2010) Enhancement of proteasome activity by a small-molecule inhibitor of USP14. *Nature* **467,** 179–184
69. Lam, Y. A., Xu, W., DeMartino, G. N., and Cohen, R. E. (1997) Editing of ubiquitin conjugates by an isopeptidase in the 26S proteasome. *Nature* **385,** 737–740
70. Hamazaki, J., Iemura, S., Natsume, T., Yashiroda, H., Tanaka, K., and Murata, S. (2006) A novel proteasome interacting protein recruits the deubiquitinating enzyme UCH37 to 26S proteasomes. *Embo J.* **25,** 4524–4536
71. Qiu, X. B., Ouyang, S. Y., Li, C. J., Miao, S., Wang, L., and Goldberg, A. L. (2006) hRpn13/ADRM1/GP110 is a novel proteasome subunit that binds the deubiquitinating enzyme, UCH37. *Embo J.* **25,** 5742–5753
72. Rosenzweig, R., Bronner, V., Zhang, D., Fushman, D., and Glickman, M. H. (2012) Rpn1 and Rpn2 coordinate ubiquitin processing factors at proteasome. *J. Biol. Chem.* **287**(18), 14659–14671
73. Aufderheide, A., Beck, F., Stengel, F., Hartwig, M., Schweitzer, A., Pfeifer, G., Goldberg, A. L., Sakata, E., Baumeister, W., and Forster, F. (2015) Structural characterization of the interaction of Ubp6 with the 26S proteasome. *Proc. Natl. Acad. Sci. U S A* **112,** 8626–8631
74. Bashore, C., Dambacher, C. M., Goodall, E. A., Matyskiela, M. E., Lander, G. C., and Martin, A. (2015) Ubp6 deubiquitinase controls conformational dynamics and substrate degradation of the 26S proteasome. *Nat. Struct. Mol. Biol.* **22,** 712–719
75. Kleijnen, M. F., Roelofs, J., Park, S., Hathaway, N. A., Glickman, M., King, R. W., and Finley, D. (2007) Stability of the proteasome can be regulated allosterically through engagement of its proteolytic active sites. *Nat. Struct. Mol. Biol.* **14,** 1180–1188
76. Lee, S. Y., De la Mota-Peynado, A., and Roelofs, J. (2011) Loss of Rpt5 protein interactions with the core particle and Nas2 protein causes the formation of faulty proteasomes that are inhibited by Ecm29 protein. *J. Biol. Chem.* **286,** 36641–36651
77. Gorbea, C., Pratt, G., Ustrell, V., Bell, R., Sahasrabudhe, S., Hughes, R. E., and Rechsteiner, M. (2010) A protein interaction network for Ecm29 links the 26 S proteasome to molecular motors and endosomal components. *J. Biol. Chem.* **285,** 31616–31633
78. Gorbea, C., Rechsteiner, M., Vallejo, J. G., and Bowles, N. E. (2013) Depletion of the 26S proteasome adaptor Ecm29 increases Toll-like receptor 3 signaling. *Sci. Signal.* **6,** ra86
79. Tomko, R. J., Jr., and Hochstrasser, M. (2013) Molecular architecture and assembly of the eukaryotic proteasome. *Annu. Rev. Biochem.* **82,** 415–445
80. Kaneko, T., Hamazaki, J., Iemura, S., Sasaki, K., Furuyama, K., Natsume, T., Tanaka, K., and Murata, S. (2009) Assembly pathway of the Mammalian proteasome base subcomplex is mediated by multiple specific chaperones. *Cell* **137,** 914–925
81. Pratt, W. B., Gestwicki, J. E., Osawa, Y., and Lieberman, A. P. (2015) Targeting Hsp90/Hsp70-based protein quality control for treatment of adult onset neurodegenerative diseases. *Annu. Rev. Pharmacol. Toxicol.* **55,** 353–371
82. Grune, T., Catalgol, B., Licht, A., Ermak, G., Pickering, A. M., Ngo, J. K., and Davies, K. J. (2011) HSP70 mediates dissociation and reassociation of the 26S proteasome during adaptation to oxidative stress. *Free Radic. Biol. Med.* **51,** 1355–1364
83. Imai, J., Maruya, M., Yashiroda, H., Yahara, I., and Tanaka, K. (2003) The molecular chaperone Hsp90 plays a role in the assembly and maintenance of the 26S proteasome. *Embo J.* **22,** 3557–3567
84. Prince, T., Shao, J., Matts, R. L., and Hartson, S. D. (2005) Evidence for chaperone heterocomplexes containing both Hsp90 and VCP. *Biochem. Biophys. Res. Commun.* **331,** 1331–1337
85. Kang, Y., Zhang, N., Koepp, D. M., and Walters, K. J. (2007) Ubiquitin receptor proteins hHR23a and hPLIC2 interact. *J. Mol. Biol.* **365,** 1093–1101
86. Andersen, K. M., Madsen, L., Prag, S., Johnsen, A. H., Semple, C. A., Hendil, K. B., and Hartmann-Petersen, R. (2009) Thioredoxin Txnl1/TRP32 is a redox-active cofactor of the 26 S proteasome. *J. Biol. Chem.* **284,** 15246–15254
87. Chuang, S. M., Chen, L., Lambertson, D., Anand, M., Kinzy, T. G., and Madura, K. (2005) Proteasome-mediated degradation of cotranslationally damaged proteins involves translation elongation factor 1A. *Mol. Cell. Biol.* **25,** 403–413
88. Kaye, F. J., Modi, S., Ivanovska, I., Koonin, E. V., Thress, K., Kubo, A., Kornbluth, S., and Rose, M. D. (2000) A family of ubiquitin-like proteins binds the ATPase domain of Hsp70-like Stch. *FEBS Lett.* **467,** 348–355
89. Lim, P. J., Danner, R., Liang, J., Doong, H., Harman, C., Srinivasan, D., Rothenberg, C., Wang, H., Ye, Y., Fang, S., and Monteiro, M. J. (2009) Ubiquilin and p97/VCP bind erasin, forming a complex involved in ERAD. *J. Cell Biol.* **187,** 201–217
90. Paraskevopoulos, K., Kriegenburg, F., Tatham, M. H., Rosner, H. I., Medina, B., Larsen, I. B., Brandstrup, R., Hardwick, K. G., Hay, R. T., Kragelund, B. B., Hartmann-Petersen, R., and Gordon, C. (2014) Dss1 is a 26S proteasome ubiquitin receptor. *Mol. Cell.* **56,** 453–461
91. Kao, A., Chiu, C. L., Vellucci, D., Yang, Y., Patel, V. R., Guan, S., Randall, A., Baldi, P., Rychnovsky, S. D., and Huang, L. (2011) Development of a novel cross-linking strategy for fast and accurate identification of cross-linked peptides of protein complexes. *Mol. Cell Proteomics* **10,** M110.002212